1 **Comparison of Corrosion and Cavitation Erosion Behaviors**

2 **between the As-cast and Friction-stir Processed Nickel**

3 **Aluminum Bronze**

4
5 *Q.N. Song,* Y.G. Zheng, [‡,*] S.L. Jiang,* D.R. Ni,** and Z.Y. Ma***
6
7
8 [‡] Corresponding author. E-mail: ygzheng@imr.ac.cn.
9 * State Key Laboratory for Corrosion and Protection, Institute of Metal Research, Chinese
10 Academy of Sciences, 62 Wencui Road, Shenyang 110016, China
11 ** Shenyang National Laboratory for Materials Science, Institute of Metal Research, Chinese
12 Academy of Sciences, 72 Wenhua Road, Shenyang 110016, China
13
14
15 **ABSTRACT**
16

17 An as-cast nickel aluminum bronze (NAB) was treated by friction-stir processing (FSP).

18 Immersion test and electrochemical measurements under cavitation erosion condition

19 were carried out to investigate the long-term and short-term corrosion behaviors of the

20 as-cast and as-FSP NAB. Cavitation erosion tests were conducted in both distilled water

21 and 3.5 wt. % NaCl solution. The immersion test indicated that the electrochemical

22 impedance of the as-FSP NAB was much higher, while there was little difference

23 between them in the short-term test. The cumulative mass loss of the as-cast NAB was

24 about 1.5 and 2 times as large as that of the as-FSP in distilled water and 3.5 wt. % NaCl,

25 respectively. The higher corrosion resistance of the as-FSP was due to the refined and

26 homogenized microstructure. Improved mechanical properties, less galvanic corrosion

27 sites attributed to the higher cavitation erosion resistance of the as-FSP NAB.

1

2   **Keywords**: Friction-stir processing; Corrosion; Cavitation erosion; Nickel aluminum

3   bronze; Deformation mechanism

4

5   **INTRODUCTION**

6

7   Nickel aluminum bronze (NAB) is one of the main materials used for making ship

8   propellers due to its high strength, fracture toughness and good resistance against

9   cavitation erosion and corrosion in seawater.[1, 2] It was reported that a protective oxide

10   film which was Al-rich in the inner region and Cu-rich in the outer region attributed to the

11   good corrosion resistance of NAB.[3, 4] NAB mainly contains 9-12 wt. %Al, ~5 wt. % Fe and

12   ~5 wt. % Ni. Large NAB propeller is generally composed of coarse Cu rich α phase,

13   several Fe or Ni rich precipitates (κ phases) and martensite or bainite β' phase.[5, 6]

14   The continuous nature of the κ_{III} phase was reported to make NAB vulnerable to

15   crevice corrosion.[7] Besides, Shrinkage porosities are inevitable in the castings.

16   Cavitation erosion is a common mode of material degradation in marine systems. It is

17   caused by the fluctuation of pressure in liquids. Bubbles form when the pressure drops

18   and collapse when the pressure rises. The liquid with the collapsing energy of the

19   bubbles impacts on the components as a micro jet or shock wave and causes

20   deformation and mass loss.[8] Many researches showed that good mechanical properties,

21   such as ultimate resilience ((ultimate tensile strength)^2/2(elastic modulus)) and fatigue

1   strength, contributed to high cavitation erosion resistance of the alloys.[9, 10]

2   Propeller rotates at a high speed in seawater where cavitation erosion and corrosion take

3   place simultaneously. A. Al-Hashem studied the cavitation erosion behavior of NAB in

4   seawater, selective phase corrosion and cavitation erosion stress in seawater were

5   reported to cause cracks in NAB.[11] In order to further improve the cavitation erosion and

6   corrosion resistance of the propellers castings, surface processing methods by means of

7   raising the hardness or homogenizing the microstructure have been conducted, such as

8   laser surface melting and alloying,[12-14] high velocity oxygen fuel (HVOF),[15-17] fusion

9   welding,[18] etc. A new approach to produce coatings on the surface by friction surfacing

10   was also explored recently. In this approach, a rotating stud made of the coating material

11   was pressed onto the substrate and a coating was deposited with the stud moving

12   towards. The cavitation erosion test results showed that friction surfacing reduced the

13   mass loss and extended the incubation period of NAB, the coating exhibited more plastic

14   behavior under cavitation erosion.[19] Besides the above methods, U.S. Naval Surface

15   Warfare Center [(1)] prior used a novel approach, friction-stir processing (FSP) to repair

16   and locally enhance the properties of large NAB propellers.[20]

17   FSP, derived from friction stir welding,[21] is an attractive solid-state processing method. It

18   starts with a rotating tool which is not consumable inserting into the component and the

19   tool is then traversed along the desired path to modify the microstructure. Since it is

[(1)] U.S. Naval Surface Warfare Center, Carderock Division, 9500 MacArthur Blvd., West
Bethesda, MD 20817-5700.

1   operated below the melting point of the materials, defects arisen by laser melting and

2   fusion welding, which are conducted above the melting point, are avoided. Poor adhesion

3   to the substrate for the coating generated by HVOF was also reported,[22] it can be

4   avoided by FSP. Effect of FSP on the microstructure, mechanical and corrosion

5   properties of Al-, Mg-, Ti- and Fe-based alloys has been investigated in many

6   researches.[23-25] Besides the improvement of the above properties, recent studies

7   showed that cavitation erosion resistance of hydraulic turbine steel was also greatly

8   improved by FSP.[26, 27] As for NAB, researches have been conducted on the

9   microstructure analysis after FSP. The mechanical properties of NAB, such as hardness,

10   tensile strength and elongation were also reported to be increased after FSP and

11   influenced by the processing parameters.[28-30] Residual stress introduced by FSP due to

12   the severe plastic deformation was also studied.[31] However the corrosion and cavitation

13   erosion resistance of NAB after FSP are not clear for lack of enough studies. It was

14   reported that there was no significant difference in the electrochemical results between

15   the NAB samples before and after FSP.[31] Our previous studies showed that corrosion

16   resistance of cast NAB was increased significantly by FSP through conducting

17   gravimetric measurements, however the polarization curves of samples before and after

18   FSP were similar.[32]

19   Based on the improved mechanical properties and homogenized microstructure, FSP is

20   also expected to improve the corrosion and cavitation erosion resistance of NAB. In the

21   present study, the corrosion and cavitation erosion behaviors of NAB UNS C95800

1   before and after FSP were investigated. The cavitation erosion deformation mechanism

2   was also discussed.

3

4   **EXPERIMENTAL PROCEDURES**

5

6   **Material and Processing**

7   A 300×70×8 mm cast NAB UNS C95800 (chemical composition in wt. %: Al 9.18, Ni

8   4.49, Fe 4.06, Mn 1.03, and Cu balance) plate was subjected to FSP, as seen in Figure

9   1[a]. The tool used was made of nickel-based alloy with the concave shoulder being 24

10   mm in diameter, threaded conical pin being 8 mm in root diameter and 6 mm in length.

11   The tilt angle of the tool was 3° during FSP. The tool rotated with a rate of 1200 rpm and

12   traversed with a speed of 50 mm/min, since a good combination of strength and plasticity

13   after FSP was achieved with these processing parameters.[29] The microstructure before

14   and after FSP were observed by metallographic microscope after etching with solution of

15   5 g $FeCl_3$ + 2 ml HCl + 95 ml C_2H_5OH. As-cast and as-FSP were used to represent

16   samples before and after FSP in the following present paper, respectively.

17   **Corrosion Tests**

18   Electrochemical measurements were carried out in a typical three-electrode glass cell

19   with a platinum foil as the counter electrode and a saturated calomel electrode (SCE) as

20   the reference electrode. Immersion tests were conducted to investigate the long-term

21   corrosion behaviors of the as-cast and as-FSP samples. Samples were immersed in 3.5

1   wt. % NaCl solution, electrochemical impedance spectroscopy (EIS) measurements

2   were performed periodically on these samples. Samples were cut from the as-cast and

3   the center of stir zone in as-FSP NAB, the sampling position in the stir zone was shown

4   in Figure 1[b]. Each of the samples was mounted in plastic tubes by two-component

5   epoxy resin with a Cu wire welded at the back, leaving an area of 0.49 cm^2 to contact the

6   solution, and ground with abrasive papers up to 1000 grit before immersion in 3.5 wt. %

7   NaCl solution. The solution which was made up from the analytical grade reagent and

8   distilled water was replaced every week to keep fresh. Electrochemical measurements

9   were also conducted under cavitation erosion condition to investigate the short-term

10   corrosion behaviors of the as-cast and as-FSP samples (the detailed sample preparation

11   and cavitation erosion condition were stated in the following part).

12   The EIS test was performed in the frequency domain of 100 kHz-10 mHz with a 5 mV

13   peak to peak amplitude for the immersion tests. For the electrochemical measurements

14   under cavitation erosion, EIS was conducted from 20 kHz to 100 mHz and the

15   polarization curves were recorded at a sweep rate of 1 mV/s from -250 mV to 250 mV

16   versus the open circuit potential.

17   **Cavitation Erosion Tests**

18   An ultrasonically vibratory apparatus was used for cavitation erosion tests. It worked at a

19   frequency of 20 kHz and an amplitude of 60 μm. The sample was fastened to a holder

20   which was set in the container filled with electrolyte and immersed 15 mm below the

21   electrolyte surface. It was right below the horn of the vibratory apparatus and the

1   distance between the horn and the sample was 0.5 mm. The electrolyte temperature was

2   maintained at about 20 °C using the cycling cooling water.

3   Samples for cavitation erosion tests were machined from the as-cast and as-FSP NAB

4   along the processing direction, the sampling position and the working surface geometry

5   were shown in Figure 1[a] and [c], respectively. They were ground with abrasive papers

6   up to 1000 grit for gravimetric measurements, and polished with diamond suspension of

7   1 μm size for morphology observation. Distilled water and 3.5 wt. % NaCl solution were

8   used as the test electrolytes. The samples were ultrasonically cleaned in ethanol, dried

9   with blowing air and weighed initially and at regular intervals using an electronic balance

10   with an accuracy of 0.1 mg. The surface and the cross-section part of the eroded

11   samples were observed by scanning electron microscopy (SEM). 3D surface morphology

12   was observed with a laser confocal microscope. All the above tests were repeated at

13   least three times in order to ensure the accuracy.

14

15   **RESULTS**

16

17   **Microstructure**

18   The microstructures of the as-cast and as-FSP NAB are shown in Figure 2. The as-cast

19   NAB is composed of coarse Widmanstätten α phase with a size of over 100 μm which

20   is lightly etched, β' phase and κ particles which are darkly etched, as seen in Figure

21   2 [a] and [b]. The stir zone of as-FSP NAB consists of heterogeneous microstructure

1   along the depth with Widmanstätten α and fine β' phases at the surface (Figure 2 [c]),

2   banded and some Widmanstätten α and β' phases at the sub-surface which is about

3   1.5 mm from the surface(Figure 2 [d]), equiaxed α and β' phases at the middle which

4   is about 3 mm from the surface (Figure 2 [e]) and stream-like α and β' phases at the

5   bottom which is about 6 mm from the surface (Figure 2 [f]). It is obvious that the grains

6   and particles in the cast microstructure are greatly refined after FSP. The Widmanstätten

7   α is less than 20μm and the equiaxed α is about 10μm in grain size. Finer α grains

8   are also found in the banded and stream-like structures, with the grain size being about

9   10 μm and 3-4 μm, respectively.

10   **Corrosion Behavior of Long-term Immersion**

11   EIS is a powerful, non-destructive technique used to explore the reactions at the

12   metal/electrolyte interface and the films or corrosion products formed on the metal. In the

13   present study, the impedance spectra were recorded after different immersion time to

14   monitor the surface change of the as-cast and as-FSP NAB. Figure 3 shows the Nyquist

15   plots. The diameter of the capacitive circle in the Nyquist plot indicates the quality of film

16   formed on the surface. Two points can be seen from Figure 3. One is that the diameter of

17   the capacitive circle increases with the immersion time for both the as-cast and as-FSP.

18   This suggests a progressive oxide film formation on the surface for both the as-cast and

19   as-FSP. The other is that the diameter of the capacitive circle increases at a much more

20   rapid rate for the as-FSP NAB. After 10 days' immersion, the diameter of the capacitive

21   circle of the as-FSP NAB is about one order of magnitude higher than that of the as-cast.

1   This indicates that the film produced on the as-FSP NAB was more protective and acted

2   as a compact barrier to the metallic dissolution. It is consistent with the results in our

3   previous study that the mass loss of the as-FSP NAB was much lower than that of the

4   as-cast through the immersion tests in 3.5 wt. % NaCl solution.[32]

5   **Cavitation Erosion Behaviors**

6   <u>**In distilled water**</u>.

7   Figure 4 shows the graphs of cumulative mass loss and cumulative mass loss rate as a

8   function of cavitation erosion time for the as-cast and as-FSP NAB in distilled water. The

9   mass loss is not obvious during the first 5 hours for both the as-cast and as-FSP. After 9

10   hours, the mass loss of the as-cast one increases rapidly, the cumulative mass loss rate

11   is nearly steady for the as-FSP while still increases for the as-cast. At the end of the test,

12   the cumulative mass loss is about 30 mg for the as-cast which is 1.5 times as large as

13   that for the as-FSP. The cumulative mass loss rate during the whole cavitation erosion

14   period is about 1.3 mg/h for the as-cast and 0.8 mg/h for the as-FSP.

15   In Figures 5-8, SEM images for the damaged surface morphologies of the as-cast and

16   as-FSP NAB after different cavitation erosion time are presented. In Figure 5, the

17   deformation of the as-cast is much more severe than that of the as-FSP after 3 hours.

18   Small and shallow cavities of the as-FSP NAB distribute evenly. While for the as-cast, the

19   cavities are much larger indicating severe deformation and mass loss. In large

20   magnification (Figure 5 [d]), there are many extrusions which indicate plastic deformation

21   for the as-FSP. While for the as-cast, cracks appear at the phase boundaries between

1   α and κ due to the cavitation erosion stress, large particles κ_{II} are totally tore off,

2   cracks are also found between the lamellas of $\alpha + \kappa_{III}$ (Figure 5 [c]). After 9 hours,

3   deformation and damage caused by cavitation erosion almost cover the whole surface

4   for both the as-cast and as-FSP NAB, as shown in Figure 6. For the as-FSP one there

5   are still no large and deep cavities which are widespread in the as-cast. At the end of the

6   cavitation erosion duration, the damaged surface of as-FSP is still relatively smooth,

7   while there are honeycombed and macroscopic cavities all over the surface of the

8   as-cast sample in Figure 7. Figure 8 shows the cross sections of the as-cast and as-FSP

9   NAB after cavitation erosion for 20 hours. For the as-cast NAB, the depth of some

10   cavities is over 150 μm (Figure 8 [a]). Many cracks forms at the periphery of the cavities,

11   a crack of about 20 μm long extending in α phase is found at the bottom of the cavities

12   (Figure 8 [c]). For the as-FSP NAB (Figure 8 [b]), the depth of the cavities is less than 10

13   μm. Long cracks are not found in Figure 8 (d). The as-FSP NAB seemed to deform just

14   below the surface.

15   **In 3.5 wt. % NaCl solution.**

16   The above tests focused on the mechanical attack, while for propeller working in natural

17   seawater, the cavitation erosion process was more complex. Corrosion, erosion and their

18   synergism caused the damage of the materials. So the cavitation erosion tests in 3.5

19   wt. % NaCl solution were also conducted to simulate the cavitation erosion condition in

20   seawater in the present study. The cumulative mass loss and mass loss rate as a

21   function of cavitation erosion time are shown in Figure 9. The cumulative mass loss in 3.5

1   wt. % NaCl solution increases for both the as-cast and as-FSP NAB compared to that in

2   distilled water. After cavitation erosion for 16 hours, the cumulative mass loss is 33.4 mg

3   and 15.9 mg for the as-cast and as-FSP in 3.5 wt. % NaCl solution, respectively and in

4   distilled water, the cumulative mass loss is 16.1 mg for the as-cast and 11.2 mg for the

5   as-FSP. The mass loss in 3.5 wt. % NaCl solution increases by 50% for the as-cast

6   compared with the result in distilled water while 25% for the as-FSP. The cumulative

7   mass loss rate after 16 hours' cavitation erosion is 2.09 mg/h for the as-cast and 1 mg/h

8   for the as-FSP in 3.5 wt. % NaCl solution,   while 1 mg/h and 0.7 mg/h for the as-cast

9   and as-FSP, respectively.

10   Figure 10 shows the damaged surface morphologies after cavitation erosion for 3 hours.

11   Compared with the results in distilled water, both the as-cast and as-FSP suffered more

12   severe damage in 3.5 wt. % NaCl solution. For the as-cast NAB, the microstructure is

13   hardly recognized since damage covers all over the surface and deep cavities are

14   obvious (Figure 10 [c]). For the as-FSP, the microstructure is visible due to the corrosion.

15   Instead of extrusions exhibited in distilled water, the collapsing of microstructure and

16   increment of small cavities are mainly found here (Figure 10 [d]). Apparently the damage

17   on the surface of as-cast is uneven and more severe than that for as-FSP.

18   The 3D morphology of the damaged surface observed by laser confocal microscope is

19   presented in Figure 11. The Z-axis was chosen according to the distance between the

20   peak and valley of the surface. After cavitation erosion for 3 hours, for the as-cast NAB,

21   the Z-axis used is 19.4 µm and some larger cavities are already visible. While for the

1   as-FSP, the Z-axis is only 9 μm and smaller cavities are distributed evenly over the

2   surface. After cavitation erosion for 5 hours, for the as-cast NAB, the Z-axis increases to

3   30 μm, the cavities grow rapidly, some cavities join together and cause great mass loss.

4   While for the as-FSP, there is subtle change in the Z-axis which indicates that few deeper

5   cavities formed, but the number of cavities increases. After cavitation erosion for 16

6   hours, for the as-cast NAB, the Z-axis is set to be 205 μm, the surface is damaged

7   severely. While for the as-FSP, the Z-axis also increases to 40 μm.

8   **The Electrochemical Measurements Under Cavitation Erosion**

9   Figure 12 [a] shows the open circuit potential evolution of alternate quiescent and

10   cavitation erosion conditions for the as-cast and as-FSP NAB. Cavitation ersoion shifts

11   the open circuit potential in the active direction for about 80 mV and 100 mV for the

12   as-cast and as-FSP, respectively. The open circuit potential increases to the value under

13   quiescent condition when cavitation erosion stops. Cavitation erosion increases the

14   current density (Figure 12 [b]) and decreases the diameter of the capacitive circle in the

15   Nyquist plots for both the as-cast and as-FSP NAB (Figure 12 [c] and [d])). With

16   increasing the cavitation erosion time, the diameter of the capacitive circle in the Nyquist

17   plots decreases. However there is little difference between the as-cast and as-FSP under

18   both quiescence and cavitation erosion conditions from the polarization curves and

19   impedance spectra results.

20

1   **DISCUSSION**

2

3   The above results clearly indicate that the as-FSP NAB possesses better corrosion and

4   cavitation erosion resistance in both distilled water and 3.5 wt. % NaCl solution than the

5   as-cast substrate.

6   **Corrosion Behavior**

7   The Nyquist plots shown in Figure 3 after long-term immersion clearly showed that the

8   electrochemical impedance of the as-FSP NAB was much higher than that of the as-cast

9   one. It suggested that the film generated on the surface of the as-FSP NAB grew rapidly

10   and was more protective. For the as-cast NAB, large κ particles and casting porosities

11   made the film discontinuous and inhomogeneous. The films formed over different phases

12   of the as-cast NAB were different in composition, structure and growth rate. Cracks

13   would appear in the film due to the growth stress caused by the inhomogeneous

14   structure and growth rate. Furthermore severe segregation at the phase boundaries, as

15   well as galvanic cells due to the potential difference of different phases, caused the

16   concentration of chloride ions there and facilitated the corrosion rate, so the film was

17   easily damaged and thinner or non-protective at these places. While FSP eliminated the

18   casting defects and modified the inhomogeneous microstructure. It was also reported

19   that FSP improved the corrosion resistance of Al alloy since it increased the dissolution

20   of CuAl$_2$ particles which would cause galvanic corrosion.[33, 34] The study of Ferrara and

21   Caton showed that the coarser microstructures of NAB resulted in a deeper attack in

1   seawater.[35] So the refined and homogenized microstructure after FSP was more

2   corrosion resistant. The surface of as-FSP NAB was uniformly corroded, so the film

3   formed was homogeneous and continuous, it grew more rapidly and was more protective

4   than that of the as-cast one. So the long-term immersion tests showed that the corrosion

5   resistance of the as-cast NAB was improved by FSP.

6   The effect of cavitation erosion on the corrosion behavior mainly depends on two

7   competing effects, namely, corrosion film or product detachment and the increase of

8   mass transport. The former shifts the potential in the active direction by exposing the

9   fresh base metal, while the latter shifts the potential in the noble direction by enhancing

10   oxygen supply to the substrate surface through severe stir under cavitation erosion. In

11   the present study, the open circuit potential was shifted in the active direction, as seen in

12   Figure 12 [a], so the former effect was the leading one. Under quiescent conditions, films

13   built up on the surfaces of both the as-cast and as-FSP NAB, however they were

14   destroyed and fresh metal surfaces were exposed under cavitation erosion conditions.

15   When cavitation erosion stopped, film rebuilt up and the open circuit potential increased

16   to the value under quiescent conditions. The current density increased and the surface

17   impedance decreased for both the as-cast and as-FSP NAB under cavitation erosion, as

18   shown in Figure 12[b], [c] and [d]. The anodic current increased for the accelerated

19   dissolution of the fresh substrate, since there was no protective film to hamper the

20   diffusion of metallic ion to the solution, and the damaged surface which was rough and

21   severely deformed provided more weak sites for the corrosion attack. The cathodic

1   current increased due to the enhanced oxygen supply to surface for oxygen reduction.

2   For both the as-cast and as-FSP NAB, the impedance decreased with increasing the

3   cavitation erosion time due to the rougher surface, more severe deformation and cavities

4   with continuous cavitation erosion attack.

5   Obviously, the corrosion behaviors of the as-cast and as-FSP NAB differed little with

6   each other under cavitation erosion condition. However it was mentionable that the

7   electrochemical test conducted under cavitation erosion condition was a short-term test,

8   only the short-term behaviors of the as-cast and as-FSP could be observed. The fresh

9   substrate surface was exposed to the corrosive solution all the time since there was no

10   protective film on it due to the continuous cavitation erosion attack, so only the original

11   behavior was investigated under cavitation erosion condition for both the as-cast and

12   as-FSP NAB. On the one hand, the refined and homogenized microstructure of as-FSP

13   was more resistant to localized corrosion compared with the coarse, inhomogeneous

14   microstructure of as-cast sample. On the other hand, the severe plastic deformation and

15   residual stress were brought about during FSP. The residual stress was reported to

16   exceed +200Mpa and -200Mpa in the direction parallel and perpendicular to the

17   processing path, respectively.[31] Lynch pointed out that the friction stir processed Mn-Cu

18   alloy without residual stress relieving suffered similar dealloying depth as the as-cast

19   sample, while the processed sample with stress relieving by heat treatment possessed

20   smaller dealloying depth than the as-cast.[36] So the residual stress might also make the

21   surface of the as-FSP NAB active and vulnerable to corrosion in the present study.

1   Therefore for the as-FSP NAB, the favorable aspect expected to raise the corrosion

2   resistance was neutralized by the detrimental one. It was resistant with the results in our

3   previous studies that there was little difference in the polarization curves and impedance

4   spectra between the as-cast and as-FSP NAB, since those tests were also short-term

5   tests which could only explore the initial behaviors.[32]

6   As for the immersion tests under quiescent conditions, the as-FSP NAB probably

7   dissolved more quickly in the initial period since the above detrimental aspect of FSP

8   made the surface active and the metal ions diffused to the solution. With increasing the

9   immersion time, the metal ions concentrated and deposited on the surface, then a film

10   was formed acting as a compact barrier and hampered the ionic transport, therefore the

11   metallic dissolution was restrained effectively. This could also explain why the film

12   impedance of as-FSP increased more rapidly than that of the as-cast.

13   **Cavitation Erosion Behavior**

14   The results that the as-FSP NAB possesses higher cavitation erosion resistance were

15   not surprising, since the mechanical properties including elongation and tensile strength

16   were reported to be highly improved by FSP according to our previous study.[29] Cavitation

17   erosion resistance was positively related to these mechanical properties. The detailed

18   deformation mechanisms under cavitation erosion for the as-cast and as-FSP NAB were

19   explained as follows.

20   In distilled water, after cavitation erosion for 3 hours, extrusions were found on the

21   surface of the as-FSP, as shown in Figure 5. This indicated that the as-FSP NAB

1   possessed good ductile behavior and it was consistent with the results of S. Hanke.[19] For

2   the as-cast NAB, different phases acted differently to the cavitation erosion stress due to

3   the structure difference,[37] so cracks primarily appeared at the phase boundaries. With

4   the collapse of the phase boundaries, κ_{II} and κ_{III} were torn off leaving large and deep

5   cavities that made the surface much rougher. After 9 hours, as seen in Figure 6, the

6   surface of the as-cast NAB was distinctly rougher than that of the as-FSP one. Cavitation

7   erosion resistance was negatively related to the surface roughness since defects as well

8   as concentrated stress was enriched on the rough surface. That was why the mass loss

9   increased rapidly for the as-cast NAB while slowly for the as-FSP one under the

10   continuous cavitation erosion attack. When the surface was damaged for both the

11   as-cast and as-FSP NAB, cracks and cavities propagated and extended differently. For

12   the as-FSP one, the fine and homogeneous microstructure of the substrate near the

13   subsurface impeded the extending of damage, while the damage extended easily since

14   the coarse and inhomogeneous microstructure of the substrate near the surface for the

15   as-cast one was less resistive. Therefore short cracks propagated close to the surface

16   for the as-FSP, while longer cracks propagated into the substrate much more deeply for

17   the as-cast, as shown in Figure 8.

18   In 3.5 wt. % NaCl solution, both the as-cast and as-FSP NAB exhibited lower cavitation

19   erosion resistance than in distilled water, as shown in Figure 9. The synergism between

20   cavitation erosion and corrosion should be concerned here. For the as-cast NAB,

1 potential difference among the multiple phases could cause galvanic corrosion. κ_{II}, κ_{IV}

2 were cathodic with respect to α phase, so α was corroded preferentially at the phase

3 boundaries close to these particles. κ_{II}, κ_{IV} would be easily torn off under cavitation

4 erosion stress with the continuous dissolution of α phase. Lamellar $\alpha + \kappa_{III}$

5 possessed inferior corrosion resistance due to the potential difference between α and

6 κ_{III}, so the lamellar structure was readily damaged for the synergism between cavitation

7 erosion and corrosion. For the as-FSP NAB, remnant β' was preferentially corroded.

8 Corrosion made the surface rough, provided weak sites for cavitation erosion damage

9 and therefore accelerated the mass loss. However the microstructure was refined and

10 homogenized after being subjected to FSP, the galvanic corrosion in the as-FSP NAB

11 was not as prominent as in the as-cast. It was why the mass loss increased by 50% for

12 the as-cast NAB while 25% for the as-FSP after cavitation erosion for 16 hours in 3.5

13 wt. % NaCl solution compared with the results in distilled water.

14

15   **CONCLUSIONS**

16

17 1) The long-term immersion tests showed that the electrochemical impedance of the

18 as-FSP NAB was much higher than that of the as-cast one, while the short-term

19 electrochemical tests under cavitation ersoion indicated little difference between the

20 as-cast and as-FSP. In the former tests, the refined and homogenized microstructure

21 attributed to a more protective film on the surface of the as-FSP NAB. While in the latter

1   tests, the substrate was exposed to the solution since there was no film on the surface

2   due to the cavitation erosion attack. The favorable aspect expected to raise the corrosion

3   resistance was neutralized by the detrimental one brought about by FSP.

4   2) The cavitation erosion resistance of the as-cast NAB was highly improved by FSP.

5   The cumulative mass loss of the as-cast was about 1.5 times in distilled water and 2

6   times in 3.5 wt. % NaCl solution as large as that of the as-FSP one. For the as-cast NAB,

7   detachment of large κ particles, large and deep cavities and long cracks caused the

8   mass loss mainly. While the as-FSP exhibited more plastic behavior, small and shallow

9   cavities and short cracks due to the improved mechanical properties. The synergism

10   between corrosion and cavitation erosion contributed to the mass loss increase in 3.5

11   wt. % NaCl solution compared with that in distilled water, it was larger for the as-cast

12   NAB since coarse and inhomogeneous microstructure provided more galvanic corrosion

13   sites.

14

15   **ACKNOWLEDGEMENTS**

16

19
20   **REFERENCES**
21
22   1. E.A. Culpan, G. Rose, Br. Corros. J.14 (1979): p.160.
23   2. A. Al-Hashem, P.G. Caceres, W.T. Riad, H.M. Shalaby, Corrosion 51, 5 (1995): p.

1 331.

2 3. A. Schüssler, H.E. Exner, Corros. Sci. 34, 11 (1993): p. 1793.

3 4. A. Schüssler, H.E. Exner, Corros. Sci. 34, 11 (1993): p. 1803.

4 5. E.A. Culpan, G. Rose, J. Mater. Sci. 13 (1978): p. 1647.

5 6. A. Jahanafrooz, F. Hansan, G.W. Lorimer, N. Ridley, Metall. Trans. A 14A (1983): p.

6 1951.

7 7. J.A. Wharton, K.R. Stokes, Electrochim. Acta 53, 5 (2008): p. 2463.

8 8. A. Karimi, J.L. Martin, Int. Metals Rev. 31, 1 (1986): p. 1.

9 9. R.H. Richman, W.P. NcNaughton, Wear 140, 1 (1990): p. 63.

10 10. W. Bedkowski, G. Gasiak, C. Lachowicz, A. Lichtarowicz, T. Łagoda, E. Macha, Wear

11 230, 2 (1999): p. 201.

12 11. A. Al-Hashem, W. Riad, Mater. Charact. 48 (2002): p. 37.

13 12. C.H Tang, F.T Cheng, H.C Man, Mater. Sci. Eng. A 373, 1-2 (2004): p. 195.

14 13. C.H. Tang, F.T. Cheng, H.C. Man, Surf. Coat. Technol. 200, 8 (2006): p. 2602.

15 14. C.H. Tang, F.T. Cheng, H.C. Man, Surf. Coat. Technol. 200, 8 (2006): p. 2594.

16 15. K.S. Park, S. Park, J. Electrochem. Soc. 158, 10 (2011): p. C335.

17 16. R.C. Barik, J.A. Wharton, R.J.K. Wood, K.S. Tan, K.R. Stokes, Wear 259, 1-6 (2005):

18 p. 230.

19 17. R.J.K Wood, A.J Speyer, Wear 256, 5 (2004): p. 545.

20 18. X.Y. Li, Y.G. Yan, Z.M. Xu, J.G. Li, Trans. Nonferrous Met. Soc. China 13, 6 (2003): p.

21 1317.

22 19. S. Hanke, A. Fischer, M. Beyer, J.F. dos Santos, Wear 273, 1 (2011): p. 32.

23 20. W. A. Palko, R.S. Fielder, P.F. Yang, Mater. Sci. Forum 426-432 (2003): p. 2909.

24 21. W. M. Thomas, E. D. Nicholas, J. C. Needam, M. G. Murch, P. Templesmith, C. J.

25 Dawes, Int. Patent 9125978.8, 1991.

26 22. J.F. Santa, L.A. Espitia, J.A. Blanco, S.A. Romo, A. Toro, Wear 267, 1-4 (2009): p.

27 160.

28 23. M. Atapour, A. Pilchak, G.S. Frankel, J.C. Williams, Corros. Sci. 52, 9 (2010): p. 3062.

29 24. R.C. Zeng, J. Chen, W. Dietzel, R. Zettler, J.F. dos Santos, M.L Nascimento, K.U

30 Kainer, Corros. Sci. 51, 8 (2009): p. 1738.

31 25. S. Jana, R.S. Mishra, J.B. Baumann, G. Grant, Acta Metall. 58, 3 (2010): p. 989.

32 26. H.S. Grewal, H.S. Arora, H. Singh, A. Agrawal, Appl. Surf. Sci. 268 (2013): p. 547.

33 27. J.D. Escobar, E.Vela´squez, T.F.A. Santos, A.J. Ramirez, D.Lo´ pez, Wear 297 (2013):

34 p. 998.

35 28. K. Oh-Ishi, T.R. McNelley, Metall. Mater. Trans. A 35, 9 (2004): p. 2951.

36 29. D.R. Ni, P. Xue, D. Wang, B.L. Xiao, Z.Y. Ma, Mater. Sci. Eng. A 524, 1-2 (2009): p.

37 119.

38 30. K. Oh-Ishi, T.R. McNelley, Metall. Mater. Trans. A 36, 6 (2005): p. 1575.

39 31. P.S. Prevey, D.J. Hornbach, D.N. Jayaraman, Mater. Sci. Forum 539-543(2007): p.

40 3807.

41 32. D.R. Ni, B.L. Xiao, Z.Y. Ma, Y.X. Qiao, Y.G. Zheng, Corros. Sci. 52, 5 (2010): p. 1610.

1   33. K. Surekha, B.S. Murty, K. P.   Rao, Surf. Coat. Technol. 202, 17 (2008): p. 4057.

2   34. K. Surekha, B.S. Murty, K. P. Rao, Solid State Sci. 11, 4 (2009): p. 907.

3   35. R.J. Ferrara, T.E. Caton, MP, 21 (1982): p. 30.

4   36. S.P. Lynch, D.P. Edwards, A. Majumdar, S. Moutsos, M.W. Mahoney, Mater. Sci.

5   Forum 426–4 (2003): p. 2903.

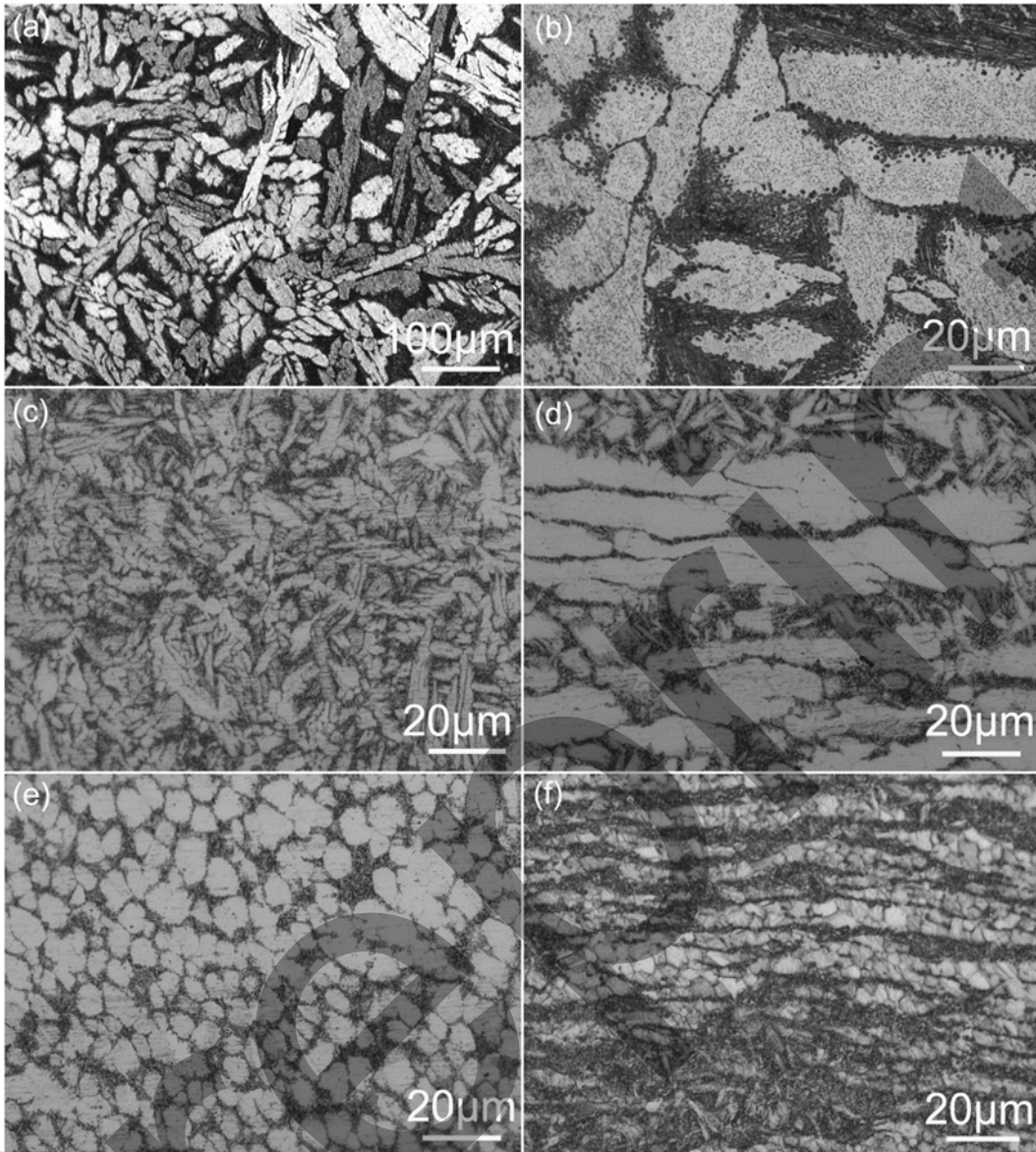6   37. F. Hasan, A. Jahanafrooz, G. W. Lorimer, N. Ridley, Metall. Trans. A 13, 8 (1982): p.

7   1337.

1
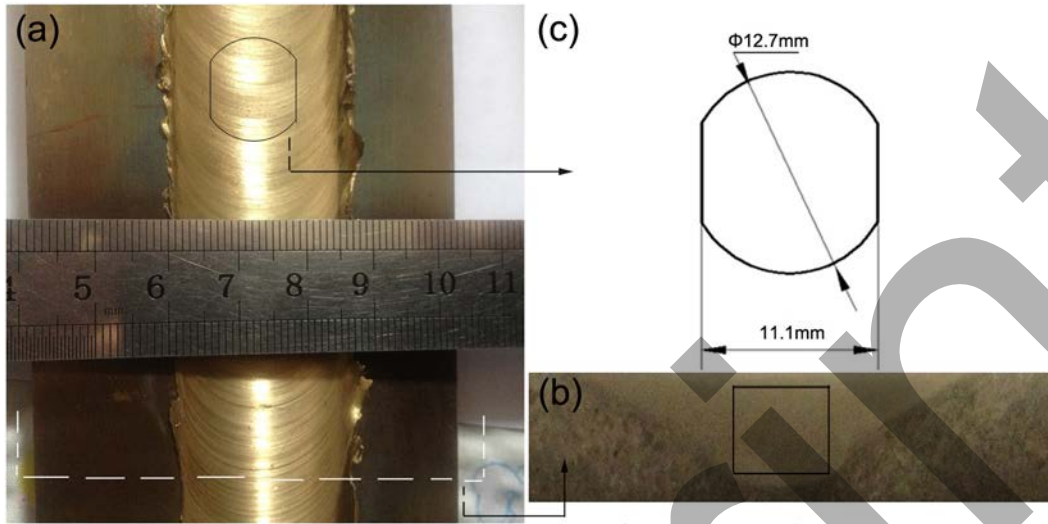
2   **FIGURES**

Song et al./Figure 1

3

4   **FIGURE 1** *(a) Top view of processed NAB; (b) cross-sectional graph of processed NAB;*

5   *(c) working surface geometry of sample for cavitation erosion test.*

6

Song et al./Figure 2

1
2 **FIGURE 2** *Microstructures of (a, b) as-cast NAB and (c-f) as-FSP NAB along the depth of*
3 *stir zone.*
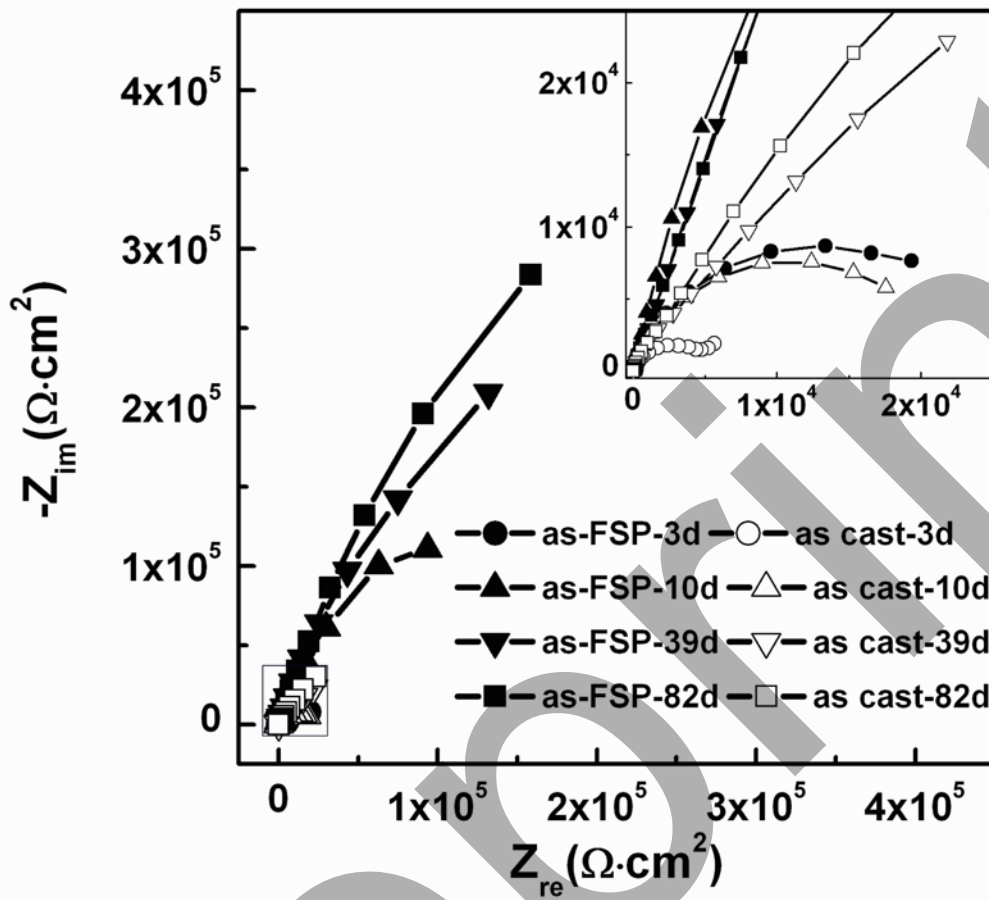
Song et al./Figure 3

1

2 **FIGURE 3** *Nyquist plots of as-cast and as-FSP NAB immersed in 3.5 wt. % NaCl solution*

3 *for different days.*

1
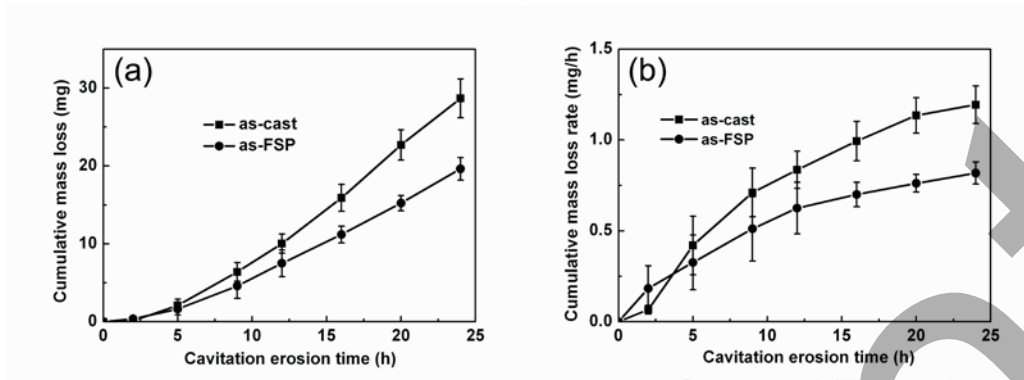
Song et al./Figure 4

2
3
4 **FIGURE 4** *Graphs of cumulative mass loss (a) and cumulative mass loss rate (b) as a*
5 *function of cavitation erosion time for as-cast and as-FSP NAB in distilled water.*

1
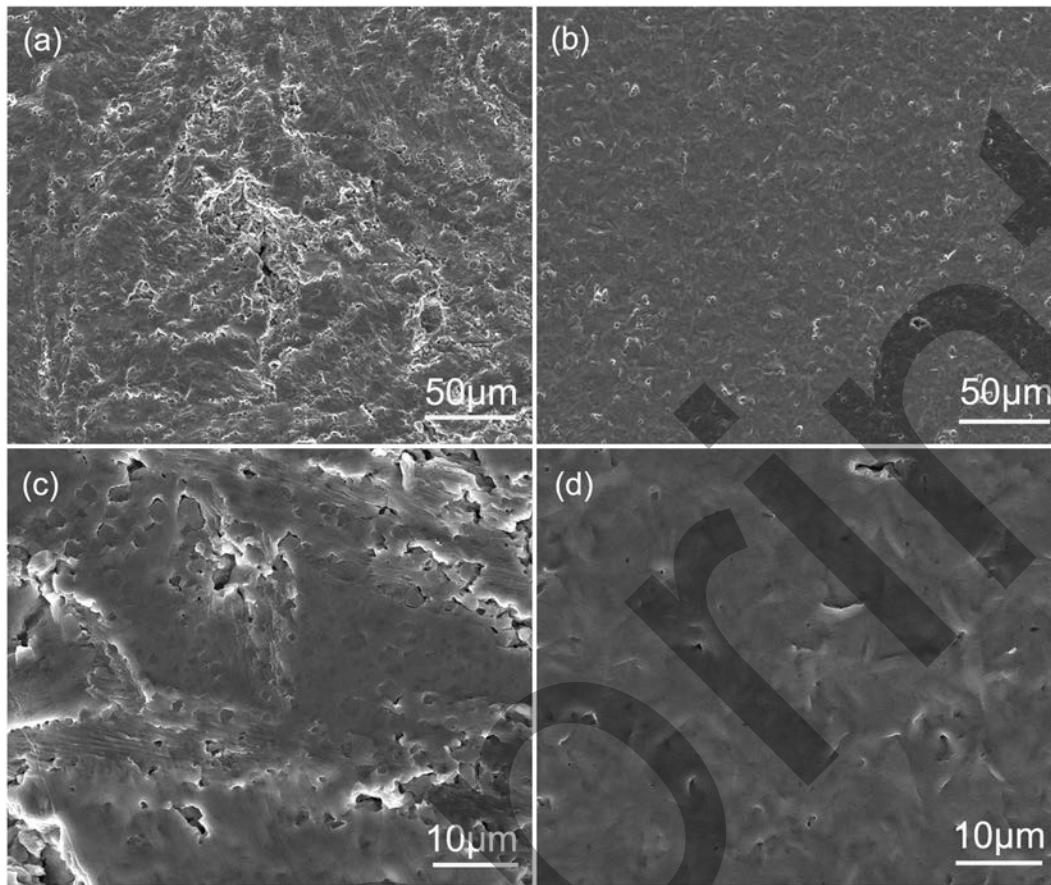
Song et al./Figure 5

2

3   **FIGURE 5** *Damage morphologies under cavitation erosion in distilled water for 3 hours:*

4   *(a , c) as-cast NAB, (b, d) as-FSP NAB.*

1
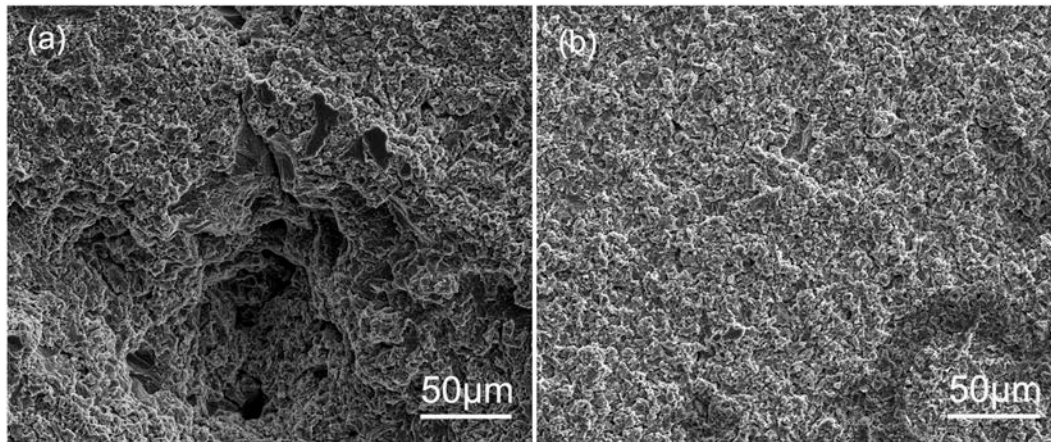
Song et al./Figure 6

2

3   **FIGURE 6** *Damage morphologies under cavitation erosion in distilled water for 9 hours:*
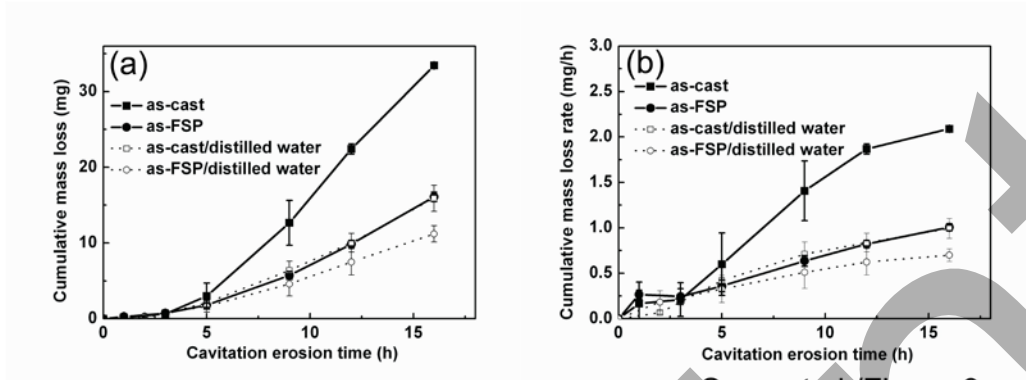
4   *(a) as-cast NAB, (b) as-FSP NAB.*

1
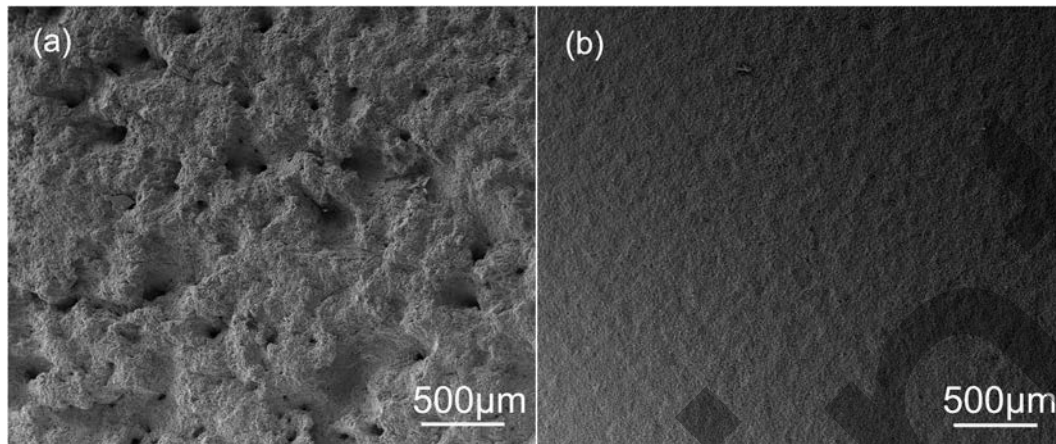
Song et al./Figure 7

2

3   **FIGURE 7** *Damage morphologies under cavitation erosion in distilled water for 24 hours:*
4   *(a) as-cast NAB, (b) as-FSP NAB.*

1
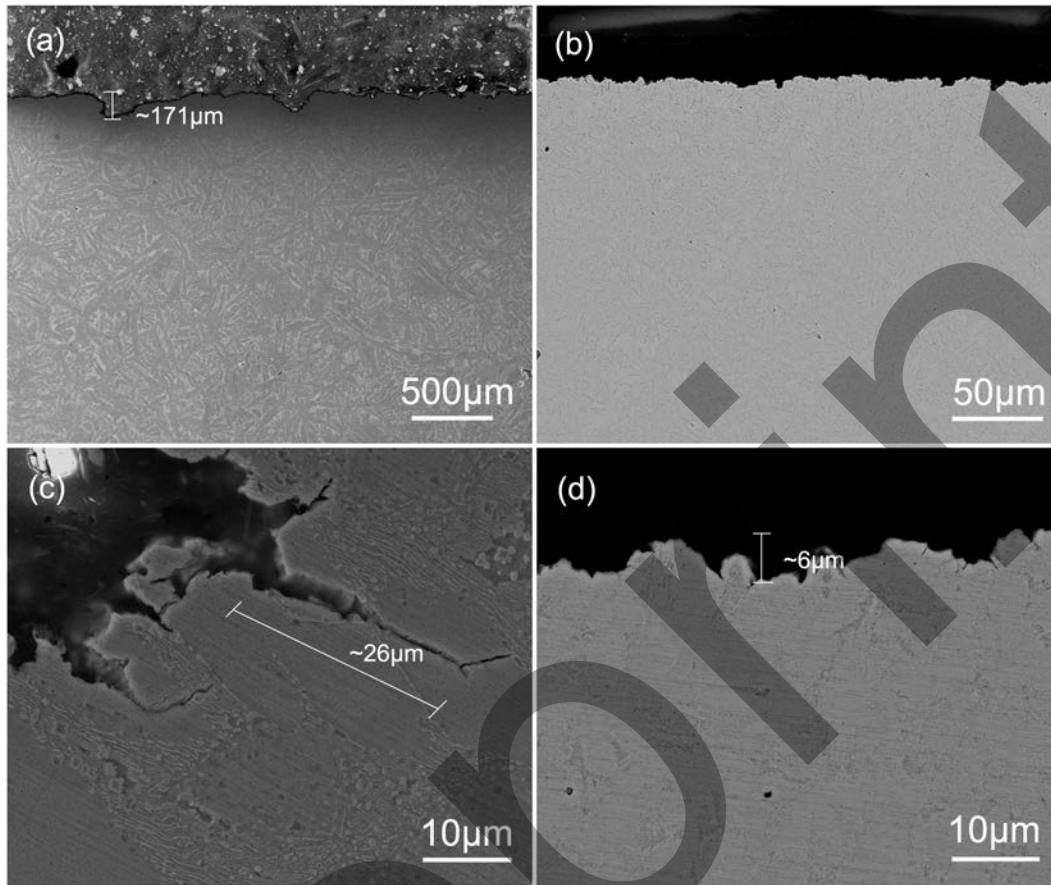
Song et al./Figure 8

2

3   **FIGURE 8** *Cross sections morphologies under cavitation erosion in distilled water for 20*
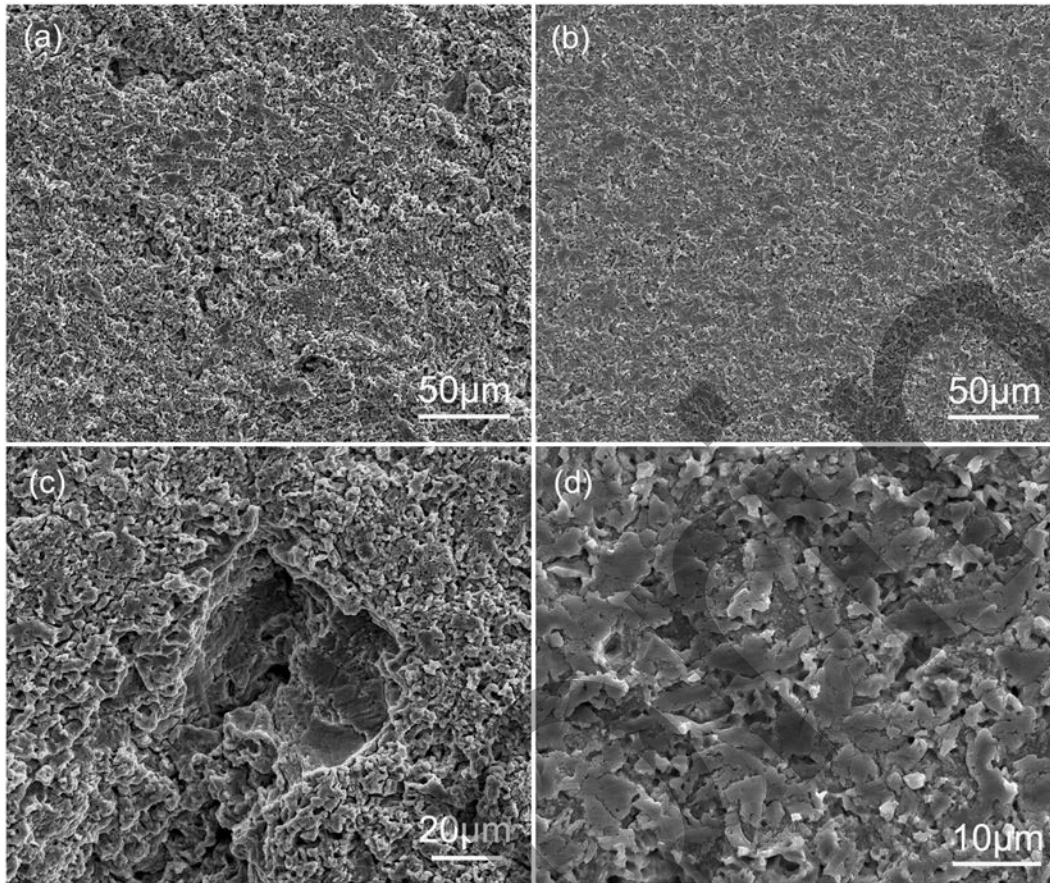4   *hours: (a, c) as-cast NAB, (b, d) as-FSP NAB.*

1

Song et al./Figure 9

2
3   **FIGURE 9** *(a) Cumulative mass loss and (b) cumulative mass loss rate as a function of*
4   *cavitation erosion time for as-cast and as-FSP NAB in 3.5 wt. % NaCl solution.*
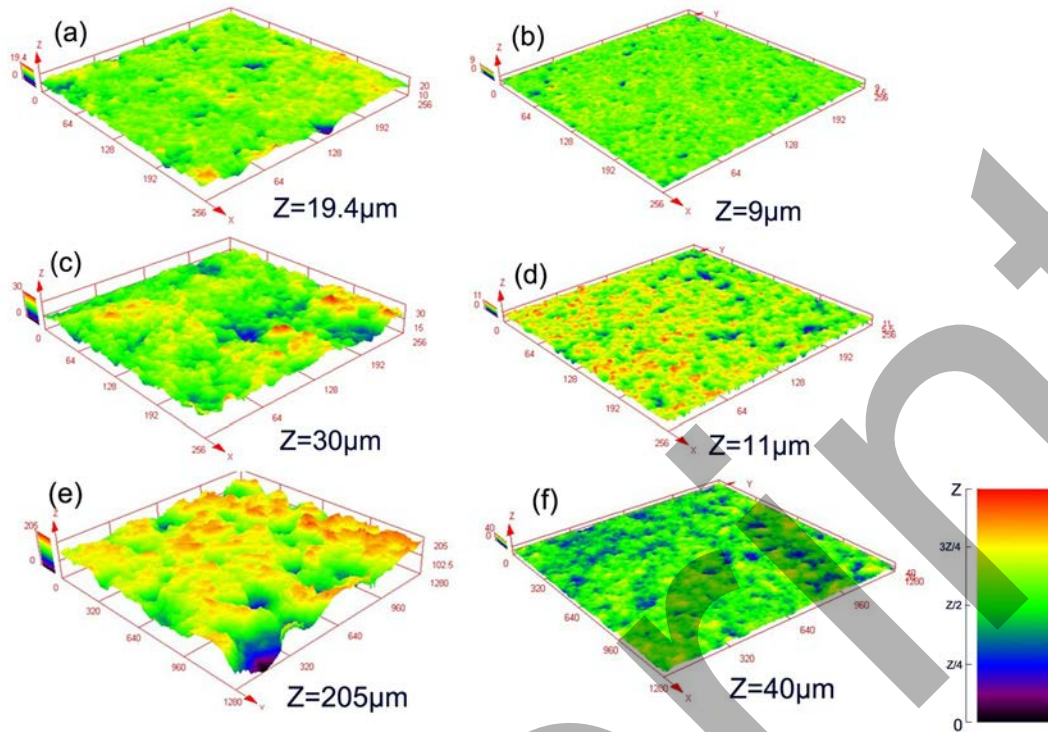
1

Song et al./Figure 10

2

3   **FIGURE 10** *Damage morphologies under cavitation erosion tests in 3.5 wt. % NaCl*
4   *solution for 3 hours: (a, c) as-cast NAB, (b, d) as-FSP NAB.*
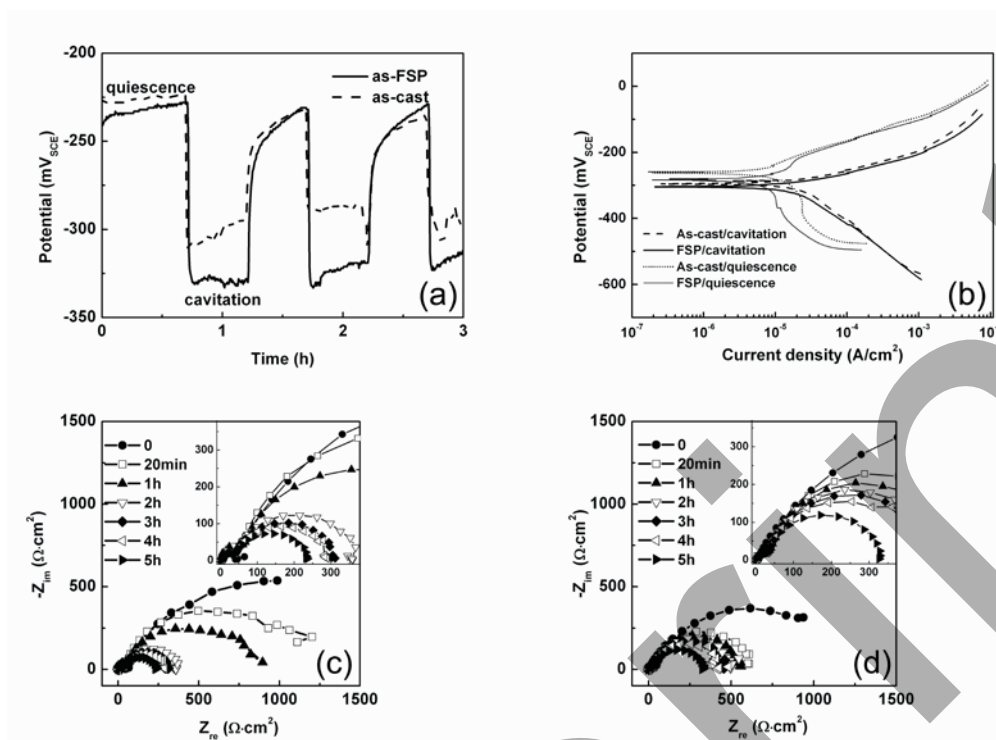
5

Song et al./Figure 11

1

2   **FIGURE 11** *3D surface morphology measured by laser confocal microscope after*
3   *cavitation erosion in 3.5 wt. % NaCl solution for: as-cast (a) 3 hours (c) 5 hours (e) 16*
4   *hours, as-FSP (b) 3 hours (d) 5 hours (f) 16 hours.*

Song et al./Figure 12

1
2
3 **FIGURE 12** *Electrochemical curves under cavitation erosion in 3.5 wt.% NaCl solution: (a)*
4 *Open circuit potential against time under alternate quiescent and cavitation erosion*
5 *conditions, (b) Polarization curves under quiescent and cavitation erosion conditions, (c)*
6 *Nyquist plots against cavitation erosion time for as-cast NAB, (d) Nyquist plots against*
7 *cavitation erosion time for as-FSP NAB.*
8